# Design of a star, planet and exo-zodiacal cloud simulator for the nulling testbench PERSEE

F. Hénault[a], P. Girard[b], A. Marcotto[a], N. Mauclert[a], C. Bailet[a], B. Lopez[a], F. Millour[a], Y. Rabbia[a], A. Roussel[a], M. Barillot[c], J. Lozi[d,g,h], F. Cassaing[d,h], K. Houairi[c], B. Sorrente[d,h], J. Montri[d,h], E. Lhomé[e,h], J.-M. Reess[e,h], L. Pham[e,h], T. Buey[e,h], V. Coudé du Foresto[e,h], S. Jacquinod[e], M. Olivier[f], J.-M. Le Duigou[g]

[a] UMR 6525 H. Fizeau, Université de Nice-Sophia Antipolis, Parc Valrose, 06108 Nice – France
[b] Observatoire de la Côte d'Azur, Boulevard de l'Observatoire, 06304 Nice – France
[c] Thales Alenia Space, 100 Boulevard du Midi, 06322 Cannes-la-Bocca – France
[d] ONERA, The French Aerospace Lab, F-92322 Châtillon – France
[e] LESIA, Observatoire de Paris, 5 Place Jules Janssen, 92195 Meudon – France
[f] IAS, Centre universitaire d'Orsay Bât 120–121, 91405 Orsay – France
[g] Centre National d'Etudes Spatiales, 18 Avenue Edouard Belin, 31401 Toulouse – France
[h] Groupement d'Intérêt Scientifique PHASE (Partenariat Haute résolution Angulaire Sol Espace) between ONERA, Observatoire de Paris, CNRS and Université Paris Diderot

## ABSTRACT

On-going developments on the PERSEE nulling testbench include the realization of a focal plane simulator featuring one central star, an extra-solar planet orbiting around it, and an Exo-Zodiacal Cloud (EZC) surrounding the observed stellar system. PERSEE (Pégase Experiment for Research and Stabilization of Extreme Extinction) is a laboratory testbench jointly developed by a Consortium of six French institutes and companies, incorporating Observatoire de la Côte d'Azur (OCA) who is in charge of the manufacturing and procurement of the future Star and Planet Simulator (SPS). In this communication is presented a complete description of the SPS, including general requirements, techniques employed for simulating the observed planet and EZC, opto-mechanical design and expected performance. The current status of the SPS activities is summarized in the conclusion, pending final integration on the PERSEE test bench in September 2011.

**Keywords:** Nulling interferometry, Nulling testbench, Exo-zodiacal cloud, Opto-mechanical design

## 1 INTRODUCTION

For more than thirty years, nulling interferometry has been one of the most studied techniques for discovering Earth-like planets orbiting around nearby stars in their habitable zone and characterizing their atmospheres [1]. It gave rise to two major space projects developed by the European Space Agency (ESA) and National Aeronautics and Space Administration (NASA), respectively named Darwin [2] and TPF-I (Terrestrial Planet Finder Interferometer [3]). Because these instruments are extremely demanding in terms of technical and operational requirements, a few intermediate class projects such as the Fourier Kelvin Stellar Interferometer (FKSI) [4] or Pégase [5] have been considered as precursors, and a laboratory test bench named PERSEE (an acronym standing for "Pégase Experiment for Research and Stabilization of Extreme Extinction") was designed, manufactured and assembled by a Consortium of six French institutes and companies, incorporating Observatoire de la Côte d'Azur (OCA). The on-going development of this nulling test bench includes the realization of a scene simulator featuring one central star, one Jupiter-like extra-solar planet orbiting around it, and an Exo-Zodiacal Cloud (EZC) surrounding the observed stellar system. In this communication is presented a complete description of the Star and Planet Simulator (SPS), including general context and requirements (§ 2), simulation of the star, planet and EZC transmission maps (§ 3.1), SPS general description (§ 3.2) and expected performance (§ 3.3), and some more detailed information about the opto-mechanical design (§ 4). Current status of the activities is summarized in the conclusion (§ 5).

Techniques and Instrumentation for Detection of Exoplanets V, edited by Stuart Shaklan,
Proc. of SPIE Vol. 8151, 815116 · © 2011 SPIE · CCC code: 0277-786X/11/$18 · doi: 10.1117/12.892748

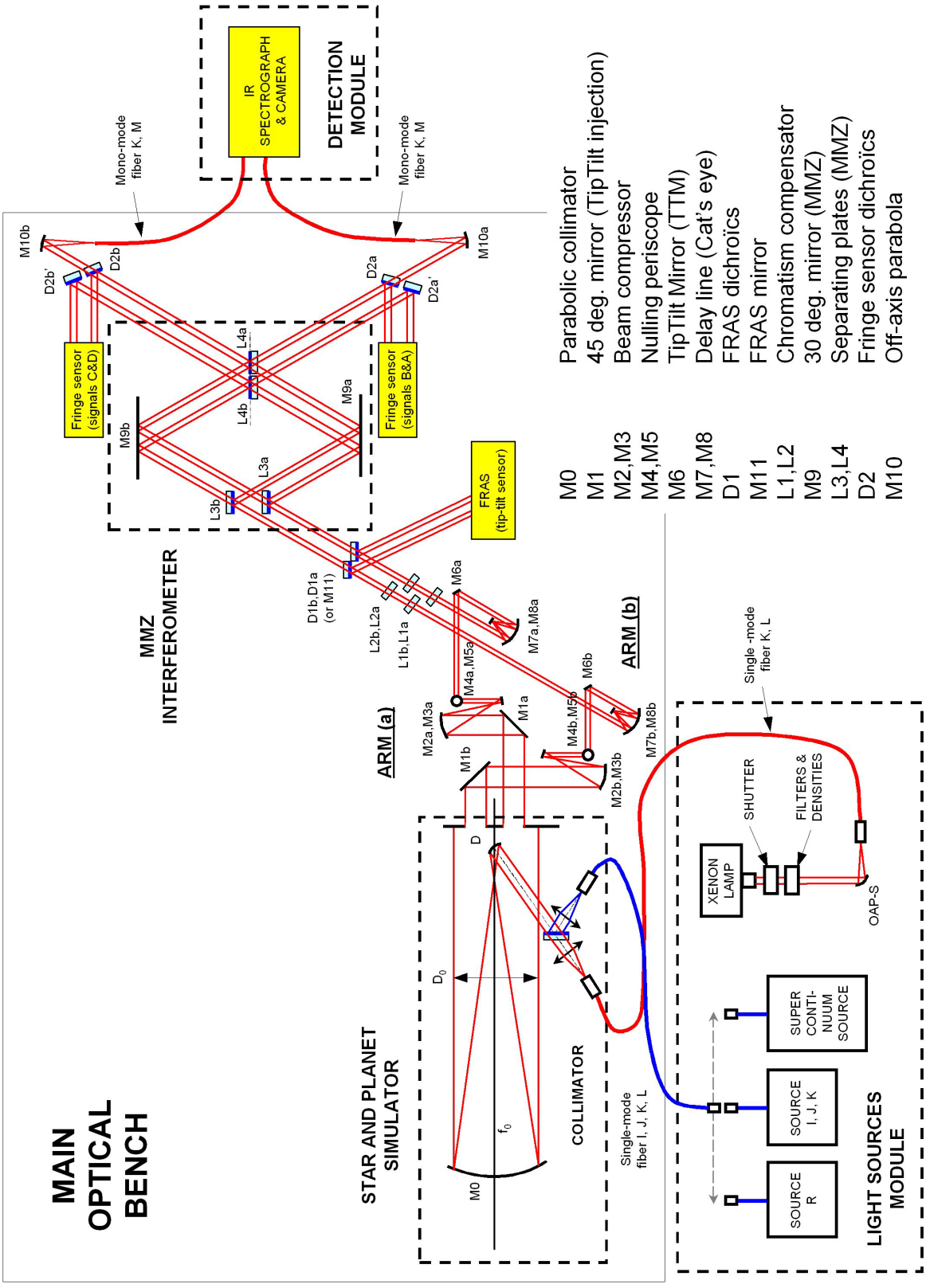


Figure 1: PERSEE general layout with upgraded star and planet simulator.

## 2 CONTEXT AND REQUIREMENTS

### 2.1 General context

The PERSEE program has been initiated and directed by the French Centre National d'Etudes Spatiales (CNES) since 2007 [6-7]. Apart CNES, the Consortium is composed of five French institutes and companies including Institut d'Astrophysique Spatiale (IAS, in charge of the Modified Mach-Zehnder combiner [8]), LESIA-Observatoire de Paris (responsible for the IR camera and final integration), Office National d'Etudes et Recherches Aérospatiales (ONERA, responsible for fringe tracker, tip-tilt sensor and software architecture), Thales Alenia Space (mechanical architecture), and OCA, who was in charge of most of the opto-mechanical components equipping the main interferometer optical train, and more especially of the star simulator module [9]. The latter activities were completed at the end of year 2009 when all OCA hardware and software were tested, validated and implemented in the clean rooms of LESIA in Meudon. Then an extensive measurement campaign began, leading to encouraging preliminary results released in summer 2010 [10], and to final results presented in another paper from this conference [11].

But in the mean time, it came out that the test bench was particularly well suited to tackle another major scientific concern, which is the presence of extra-solar debris disks similar to our own zodiacal dust disk within the observed planetary systems, and are commonly referred to as "exozodi" disks or clouds [12-13]. Their emission is a crucial parameter for preparing future projects such as Darwin/TPF-I: in our solar system, the "local" zodiacal light (hereafter defined as 1 zodi) is the brightest object after the sun. Detecting earth-sized planets in the habitable zone might be very difficult if the EZC is much brighter than our own zodiacal emission. Moreover, these exo-zodiacal discs are not well known since current instruments (for example ground based) are not sensitive enough to measure their intensity levels below 100 zodis. The envisaged approach for detecting EZCs and mapping their spatial and geometrical distribution foresees the use of multi-chromatic information, reinforcing the image reconstruction process and allowing for characterization of dust properties in their stellar environment. This approach should be necessary for FKSI or Pégase since they only comprise two sub-apertures, thus producing very sparse angular frequency coverage. Hence studying the feasibility of image reconstruction of some typical EZC scenes with a two-telescope instrument becomes a core issue, and led to a decision to upgrade the current star simulator feeding the PERSEE interferometer.

### 2.2 PERSEE optical layout

The detailed optical and mechanical design of the PERSEE nulling interferometer has already been described in previous publications (see e.g. Refs. [6-9]) and is schematically illustrated on Figure 1. Although the present paper essentially addresses the design of the light sources and SPS modules (sketched on the right side of the Figure), a few important features of the main optical train are briefly summarize here:

- PERSEE has the ability of correcting internal Optical Path Difference (OPD) between the interferometer arms and tip-tilt errors in closed loop, by means of a fringe sensor (FS) and a tilt-tilt sensor (FRAS) respectively driving two cat's eye delay lines (made of mirrors M7a-M8a and M7b-M8b on Figure 1) and a couple of tip-tilt mirrors (noted M6a and M6b) allowing stable measurement periods of several minutes. In addition, external OPD and tip-tilt errors representative of the Pégase free-flying spacecrafts or of the FKSI connected structure deformations can easily be introduced by means of the 45-deg. tilted flat mirrors M1a and M2a, and compensated for in real time. This makes PERSEE a very versatile tool suitable for testing many types of future interferometric space or balloon borne missions.
- PERSEE also includes two beam compressors (depicted as concave mirrors M2a-M3a and M2b-M3b on Figure 1) that can be used to adjust the diameter D of the useful sub-pupil at the output plane of the collimator, and therefore to work with different B/D ratios, where B is the entrance baseline of the interferometer. Hence either a long baseline (B/D = 11) or a short baseline (B/D = 3.67) instrument can be simulated using the test bench.
- Because it is only a two-arm interferometer, PERSEE does not offer the capacity to simulate rotations of the observed objects (planet, exo-zodiacal cloud) around the central star by means of OPD modulation[1], like in other multi-aperture experiments [14]. Hence the planet and EZC component will need to be actually moved at the SPS focal plane in order to represent the azimuthal rotation of the interferometer in space (see the SPS requirements in the next section).

[1] Since this would destroy the central null.

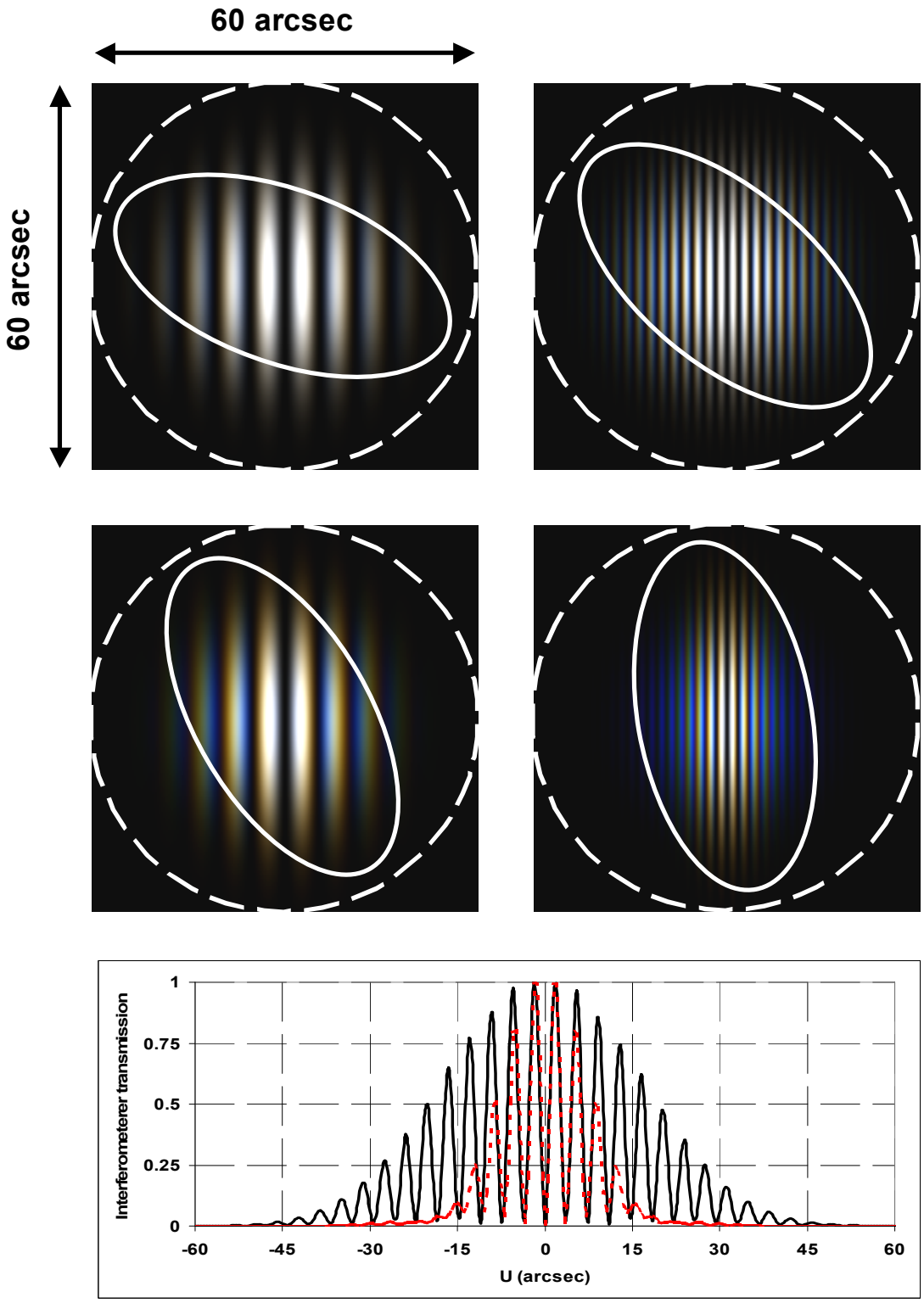


Figure 2: Illustrating PERSEE interferometer nulling maps. Top and middle rows: polychromatic transmission maps simulated for B/D = 3.67 (left column, compressing optics being installed) and B/D = 11 (right column, no compressing optics). Bottom row: slices along the baseline axis of the interferometer for B/D = 11.

### 2.3 Star and Planet Simulator (SPS) requirements

The technical requirements of the SPS have been largely modified with respect to the specification of the original star simulator presented in Ref. [9]. The main functions of the SPS are now the following:

1) To simulate a bright, unresolved star radiating from 0.6 to 3.3 μm at the entrance of the PERSEE interferometer, whose light should be extinguished by a nulling ratio lower than $10^{-4}$ and stabilized within $10^{-5}$ in the full astronomical bands H, K and L. Shorter wavelengths from 0.6 to 1.65 μm shall be used for metrology purposes (OPD and tip-tilt control).
2) To simulate an extra-solar planet orbiting around the central star, whose relative flux ratio with respect to the star could vary from $10^{-6}$ to $10^{-4}$ in the H, K and L bands, and whose angular distance to the star shall be adjustable within a limited range.
3) To simulate the presence of an extra-solar zodiacal cloud (exo-zodi) of relative flux ratio from $10^{-6}$ to $10^{-3}$ with respect to the central star, ideally represented as an elliptic background centered on the star in the same bands.

Additional requirements such as the need for auxiliary light sources, spatial filtering of the beams in order to cancel leakage from the central star, or the ability to chop, attenuate or block the beams have also been mentioned in Ref. [9]. The main geometrical requirements of the SPS are summarized in Table 1. It must be emphasized that the Field of View (FoV) characteristics, in particular, are primarily sized to some basic parameters of the existing test bench (wavelength range, interferometer baseline) rather than to realistic astronomical targets. Likewise, the radiometric characteristics of the EZC, although looking unrealistically high in those wavebands, have been extrapolated from the thermal infrared range where they are dominant.

| REQUIREMENTS | VALUES |
|---|---|
| Entrance baseline B | 110 mm |
| Entrance sub-apertures diameter D | 10 or 30 mm |
| Maximal FoV (or star/planet separation) | ± 50 arcsec |
| Star/planet distance range | Adjustable within ± 1 arcmin along two perpendicular directions |
| Planet distance accuracy and stability) | 0.25 and 0.005 arcsec |
| EZC shape | Elliptic with 50 arcsec major axis |
| Orientation of EZC major axis | Adjustable from 0 to 90 degs. by steps of 10 degs |
| EZC/star centring (accuracy and stability) | 0.5 and 0.005 arcsec |
| Collimator focal length | 750 mm |

Table 1: Main functional requirements of the SPS.

## 3 DESIGN DESCRIPTION AND PERFORMANCE

In this section are briefly presented the expected nulling maps of the interferometer (§ 3.1), the general description of the SPS (§ 3.2) and a summary of its expected radiometric and geometrical performance (§ 3.3).

### 3.1 Interferometer transmission maps

The theoretical expression of the transmission maps of a two-telescope, Bracewell fibered interferometer such as PERSEE can be deduced from previous publications [15-17]. Following their formalism it may be written as:

$$T(\mathbf{s}) = \left| \sin(\pi\, \mathbf{s}\, \mathbf{B}/\lambda) \times \left[ \hat{B}_D(\mathbf{s}) \otimes G(\mathbf{s}) \right] \right|^2, \quad (1)$$

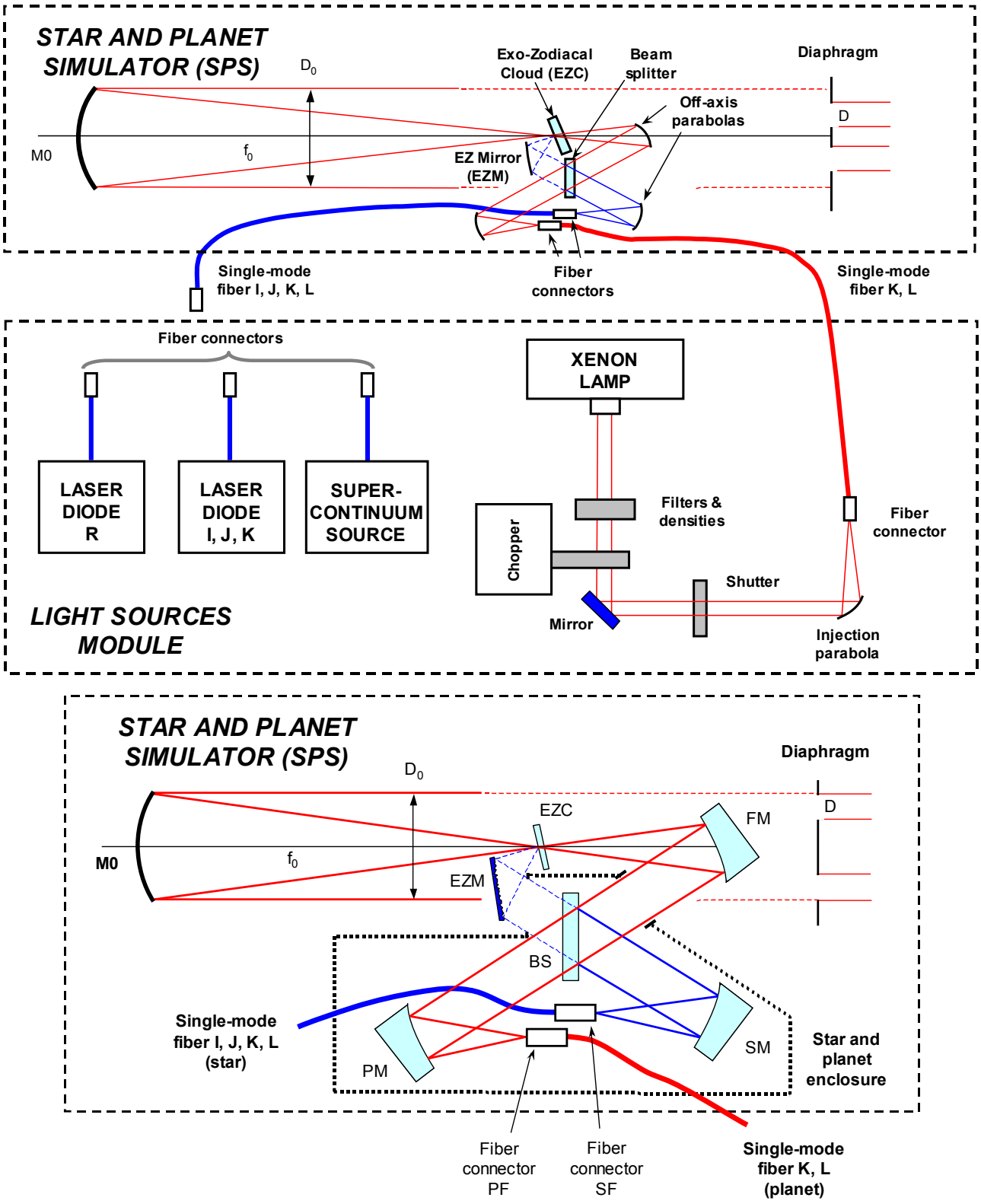


Figure 3: SPS optical layout.

where the following notations are employed:

- **s** is a unitary vector directed along any point in the object space of the interferometer (i.e. at the exit of the SPS). By definition **s** = **0** along the optical axis, where the central star is assumed to be located and nulled,
- **B** is the baseline vector joining both sub-apertures of the interferometer,
- $\lambda$ is the wavelength of the electro-magnetic field,
- $\hat{B}_D(\mathbf{s})$ is the complex amplitude generated by an individual sub-aperture and being back-projected onto the sky. For unobstructed pupils as in PERSEE, it is equal to $2J_1(\rho)/\rho$, where $\rho = \pi D \|\mathbf{s}\| / \lambda$ and $J_1$ is the type-J Bessel function at the first order,
- G(**s**) is the fundamental mode of the exit filtering waveguide, after being projected back on-sky. It can be approximated by a Gaussian function whose 1/e-radius should be equal to 0.71 $\lambda$/D in order to maximize coupling efficiency into the exit Single Mode Fibers (SMF) at the wavelength $\lambda$ [18].

Integrating Eq. 1 from $\lambda = \lambda_0 - \delta\lambda/2$ to $\lambda = \lambda_0 + \delta\lambda/2$, where $\lambda_0$ is the central wavelength and $\delta\lambda$ is the full spectral bandwidth allows computing "polychromatic nulling maps" such as presented in Figure 2. For those simulations are assumed $\lambda_0 = 2$ µm (an approximate central wavelength for both the H and K bands) and $\delta\lambda = 0.2$ µm (corresponding to an individual PERSEE spectral channel, top row of Figure 2) or $\delta\lambda = 0.75$ µm (full H+K bands, middle row in Figure 2). White solid lines are indicating the shape of some typical EZC backgrounds that will be added to the observed scenes, while dashed lines show the maximal excursion of simulated extra-solar planets.

### 3.2 Star and planet simulator module

The general optical scheme of the SPS is presented in Figures 3 and 4. It is constituted of the four main opto-mechanical sub-subsystems described in the following sub-sections.

#### *3.2.1 Light sources module*

With respect to its previous version [9], the design of PERSEE's light source module has significantly evolved during the last months in order to improve the radiometric performance of the test bench, on the one hand, and to provide the additional, necessary planet and EZC beams of light, on the other hand. The new scheme selected for simulating the central star is illustrated in Figure 4. The major modification consisted in replacing the original 75-W Xenon lamp feeding the star fiber with a super-continuum laser source (Fianium™ model SC450-2), whose optical power and radiance are assumed to be $10^5$ to $10^6$ higher. The new source is equipped with an exit Photonic Crystal Fiber (PCF) generating a perfectly single-mode and non polarized diverging light beam from 0.46 to 2.4 µm. The beam is further collimated by an Off-Axis Mirror (OAM), passes through the general shutter of the test bench, and is focused on a conveying SMF by another OAM.

Owing to its wide spectral range, the super-continuum source is routinely used to feed both the science channel (above 1.65 µm) and metrology channels of PERSEE in charge of tip-tilt sensing and fringe tracking (from 0.8 to 1.5 µm [6]). But this principal source can also be replaced with a set of three auxiliary laser diodes used for characterization purposes: to the already existing I and J laser diodes (Thorlabs at 830 nm and Exalos at 1320 nm [9]) was recently added a K band laser diode (Nanoplus at 2322 nm) allowing measurements of very deep monochromatic nulls. The K and IJ light beams are mixed together by a dichroïc plate identical to those already installed at the output of the main optical train. A red laser diode is also available for visual alignment purposes.

Finally, it must be noticed that the original Xenon lamp is now being used as the planet light source, since its flux and radiance ratios with respect to the super-continuum source seemed to be very similar to typical planet/star ratios. The accessories and feeding optics of the Xenon lamp into its own SMF are essentially the same than those already described in Ref. [9].

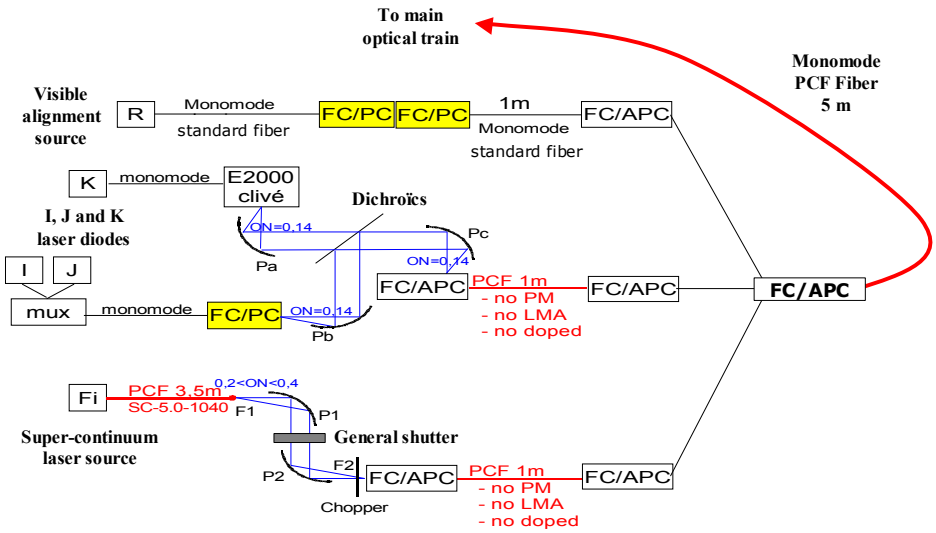


Figure 4: PERSEE's upgraded light sources module.

### *3.2.2 Light conveying fibers*

All SMFs feeding the main optical train from the light sources module to the focus of the collimator M0 have also undergone significant changes for the sake of simplicity and ease of use. The former three-fiber connector joining the science and metrology SMFs side by side at the M0 focus has been replaced with a single, 5-m length PCF (from MKT, ref. LMA-5) ensuring perfect single-mode filtering for the full science and metrology spectral bands. The mode field diameter of this fiber is around 4 µm and its numerical aperture is varying linearly with the wavelength λ, being about 0.4 in the K band. Moreover, two extra 1-m fibers were added for easy connection/disconnection with either the super-continuum or IJK light sources (see Figure 4). All the PCF fibers (also including a fourth one connecting the Xenon lamp to the planet port of the SPS) are equipped with FC/APC connectors at both ends. This ensures maximal flexibility of the test setup, since any three of the super-continuum, Xenon or diode K light sources can be connected to any of the two entrance ports of the SPS (see the next sub-section).

### *3.2.3 Star and planet mixing optics*

The star and planet mixing optics essentially form the heart of the new SPS (also comprising the collimator M0), and their components are schematically illustrated in the lower panel of Figure 3. Both heads of the "star" and "planet" fibers (respectively denoted SF and PF) are placed at the focus of two off-axis parabolic mirrors (SM and PM) of 46.6 mm focal length and coated with unprotected gold as all other mirrors in PERSEE optical train. Those mirrors are collimating the two exit beams towards a beam splitting plate (BS) where they are optically mixed. The beamsplitter is made of a simple uncoated CaF2 plate nominally reflecting 3 % of the stellar flux and transmitting 97 % of the planet flux in order to attain a typical contrast of $10^{-4}$ (see § 3.3.1).

The celestial motion of the extra solar planet with respect to its central star could naturally be realized by means of tilt adjustments of the BS plate. It might be preferable, however, to use the lateral translations of the PCFs heads that could be more easily motorized at a later stage. It must be emphasized that the design of both couples of components SF/SM and PF/PM (including mirrors, mounts and adjustment stages) is strictly identical, thus providing the same alignment capacity for both sources and ensuring full interchangeability for the star and planet beams. After being mixed, the latter are finally re-imaged at the focal plane of mirror M0 by a parabolic off-axis focusing mirror (FM) having the same focal length and reflective coatings than the SM and PM[1], but whose diameter had to be reduced to 8 mm in order to avoid any vignetting of the entrance sup-pupils of the interferometer. The beams finally cross the focal plane of the collimator, where is located a set of removable glass plates simulating the expected EZC geometries.

[1] Hence the three mirrors could be cut from the same mother parabola.

### *3.2.4 Simulating the exo-zodiacal cloud*

Adding an EZC to our now existing couple of star and planet probably is the trickiest issue of the present SPS design. In order to avoiding direct emissive solutions in the K band, or a reflective solution requiring the implementation of an auxiliary light source of the super-continuum or Xenon type, we finally decided to reuse the lost fraction of the starlight beam transmitted by the BS inside the mixing optics. This solution can be easily realized by setting a mirror of standard optical quality (named Exozodi Mirror – EZM) behind the BS plate and concentrating the beam on a small area of roughly 1 $mm^2$ at the M0 focal plane, where different EZC glass plates will be installed. Those plates should be the scope of a very specific design depicted in Figure 5: the core element is a central elliptic diffusing area, of major axis near 200 µm and having an albedo of typically 5-10 %. This ensures that light diffused from the EZC is spread over the whole M0 surface, and then to both input sup-apertures of the interferometer. The diffusing spot is surrounded by a circular, anti-reflective coated area of 200-µm diameter corresponding to the maximal planet excursion. The whole coated area (diffusive and anti-reflective) is finally limited by a fully absorptive material of at least 1 mm width in order to block stray-light eventually emitted by the mixing optics enclosure. It is currently planned to manufacture three different EZC plates, with elliptical ratio equal to 1, 0.5 and 0.25.

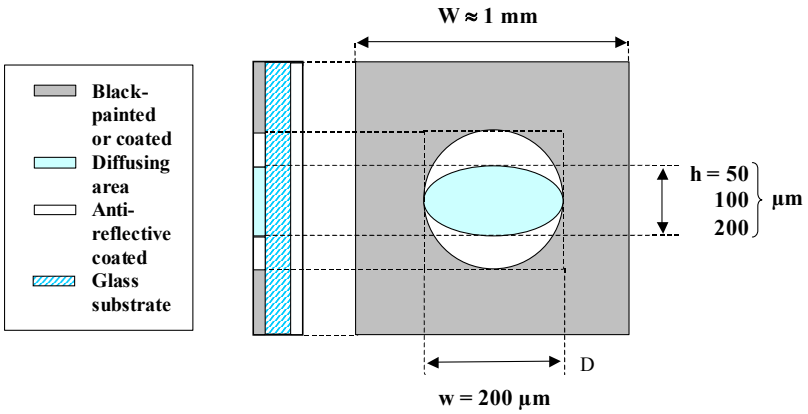


Figure 5: Tentative design of an EZC plate.

The selected EZC plates will be mounted on a three-axis translation stage: lateral displacements will serve for centering the EZC on the M0 optical axis, while the axial shift may be used to "soften" the cloud edges in some simulated astrophysical scenes. Furthermore, elliptic EZCs will need to be rotated around the main optical axis, in order to mimic the rotation of the interferometer with respect to its sky target (see Figure 2).

## 3.3 Expected performance

In this section are briefly presented the expected radiometric performance of the whole SPS (§ 3.3.1) and its main geometrical alignment requirements (§ 3.3.2).

### *3.3.1. Radiometric performance*

The expected radiometric performance of the whole SPS (from the light sources located on a remote optical bench to the entrance of the PERSEE interferometer, including light conveying SMFs, star, planet and exozodi mixing optics, and the M0 collimator) required to establish a compete radiometric budget, of which a typical example is reproduced in Table 2. From left to right, three columns are indicating the main geometrical and energetic characteristics of the optical chains, respectively for the star, planet and EZC beams. Final performance in terms of input irradiance on the interferometer pupil plane and flux ratio is given in the three last rows. This Table also illustrates two major capacities of the PERSEE test bench when the SPS will be in operation:

- The presented design allows simple modifications of some radiometric parameters (indicated by black cells in Table 2) that are useful for tuning the final flux ratios. Those are essentially the coupling efficiency of the star and planet light beams into their individual PCFs (that can be reduced by simply defocusing the fiber heads),

and a set of neutral density filters located upstream the EZC in order to attenuate the starlight flux transmitted by the uncoated BS (not shown on Figure 3). Hence fine or coarse adjustments of the star, planet and EZC intensities are easily feasible.

- As mentioned in § 3.2.3, the nominal SPS configuration foresees that the uncoated BS transmits the planet beam, while the starlight is being reflected. But exchanging both SF and PF at the input ports of the mixing optics can produce very different, alternative flux ratios indicated in the last row of Table 2. Examining these numbers, it seems remarkable that PERSEE could so easily be turned from an FKSI-Pégase prototyping experiment searching for hot Jupiters and bright EZCs into a TPF-I/Darwin-like configuration with Earth-like planets and zodiacal disks similar to our own local one.

| **STAR** | | **PLANET** | | **EXO-ZODI** | |
|---|---|---|---|---|---|
| **Super-continuum source** | | **Xenon source** | | **Super-continuum source** | |
| Spectral bandwidth | 400 nm | Spectral bandwidth | 400 nm | Spectral bandwidth | 400 nm |
| Spectral power density | 1 mW/nm | Blackbody temperature | 5800 K | Spectral power density | 1 mW/nm |
| Integrated optical power | 0.4 W | Emissivity | 0.5 | Integrated optical power | 0.4 W |
| Numerical aperture at 2.2 µm | 0.39 | | | Numerical aperture at 2.2 µm | 0.39 |
| Mode field diameter | 4.4 µm | | | Mode field diameter | 4.4 µm |
| Integrated brightness | 1.8E+10 W/m2/sr | Integrated brightness | 2.3E+05 W/m2/sr | Integrated brightness | 1.8E+10 W/m2/sr |
| **Super-continuum injection optics** | | **Xenon source injection optics** | | **Super-continuum injection optics** | |
| OAM P1 reflectivity | 0.97 | | | OAM P1 reflectivity | 0.97 |
| Shutter | 1 | Shutter | 1 | Shutter | 1 |
| K filter | 0.92 | K filter | 1 | K filter | 0.92 |
| OAM P2 reflectivity | 0.97 | Injection parabola | 0.97 | OAM P2 reflectivity | 0.97 |
| SMF coupling loss | **0.8** | SMF coupling loss | **0.8** | SMF coupling loss | **0.8** |
| Input Fresnel loss | 0.96 | Input Fresnel loss | 0.96 | Input Fresnel loss | 0.96 |
| Overall transmittance | 0.66 | Overall transmittance | 0.74 | Overall transmittance | 0.66 |
| **Photonic crystal fibers (PCF)** | | **Photonic crystal fibers (PCF)** | | **Photonic crystal fibers (PCF)** | |
| 1-m PCF attenuation | 1 | | | 1-m PCF attenuation | 1 |
| FC/APC connector | 0.9 | | | FC/APC connector | 0.9 |
| 5-m PCF attenuation | 1 | 5-m PCF attenuation | 1 | 5-m PCF attenuation | 1 |
| Output Fresnel loss | 0.96 | Output Fresnel loss | 0.96 | Output Fresnel loss | 0.96 |
| Mode field diameter | 4.4 µm | Mode field diameter | 4.4 µm | Mode field diameter | 4.4 µm |
| Mode field area | 1.5E-11 m2 | Mode field area | 1.5E-11 m2 | Mode field area | 1.5E-11 m2 |
| Overall transmittance | 0.86 | Overall transmittance | 0.96 | Overall transmittance | 0.86 |
| **Star and planet mixing optics** | | **Star and planet mixing optics** | | **Star and EZC mixing optics** | |
| SM reflectivity | 0.97 | PM reflectivity | 0.97 | SM reflectivity | 0.97 |
| BS reflectivity | 0.03 | BS transmittance | 0.97 | BS transmittance | 0.97 |
| FM reflectivity | 0.97 | FM reflectivity | 0.97 | EZM reflectivity | 0.95 |
| EZC transmittance | 0.9 | EZC transmittance | 0.9 | Neutral density | **0.01** |
| | | | | EZC albedo | 0.1 |
| | | | | SM focal length | 46.6 mm |
| | | | | EZM diameter | 8 mm |
| | | | | EZC useful diameter | 200 µm |
| | | | | EZC maximal diameter | 1 mm |
| Overall transmittance | 0.03 | Overall transmittance | 0.82 | Overall transmittance | 8.9E-04 |
| | | | | Flux collected by EZC | 7.9E-05 W |
| **M0 collimator** | | **M0 collimator** | | **M0 collimator** | |
| M0 focal length | 750 mm | M0 focal length | 750 mm | M0 focal length | 750 mm |
| Sub-pupil diameter | 10 mm | Sub-pupil diameter | 10 mm | Sub-pupil diameter | 10 mm |
| Effective numerical aperture | 0.01 | Effective numerical aperture | 0.01 | Effective numerical aperture | 0.01 |
| M0 reflectivity | 0.97 | M0 reflectivity | 0.97 | M0 reflectivity | 0.97 |
| Irradiance on sub-pupil | 2.7E-02 W/m2 | Irradiance on sub-pupil | 1.4E-05 W/m2 | Irradiance on sub-pupil | 5.6E-05 W/m2 |
| **Nominal flux ratio** | | **Planet/Star** | **5.E-04** | **Exozodi/Star** | **2.E-03** |
| **Alternative flux ratio** (exchanging SF and PF) | | **Planet/Star** | **5.E-07** | **Exozodi/Star** | **2.E-06** |

Table 2: Radiometric budget of simulated sky objects in the K band.

### *3.3.2. Alignment budget*

Alignment and stability specifications for all components of the mixing optics and the EZC plate are summarized in Table 3. Most of them were computed using ray-tracing analyses, taking into account the basic requirements expressed in Table 1, but also some other ones expressed at PERSEE interferometer level (e.g. exit optical axis misalignment ≤ 1 arcsec, decenter of the exit pupil in interferometer entrance plane ≤ 1 mm, or maximal defocus on SMF heads ≤ 10 µm).

The most stringent requirements are probably related to instabilities generated by fluctuations of the thermal environment. They could be met however, because the main PERSEE optical bench is installed into an extremely well isolated enclosure, on the one hand, and all components of the mixing optics will be integrated on a common stainless steel breadboard, on the other hand (see the CAD views of the SPS in the following section). For all tip-tilt movements, we utilize a customary system of kneecaps ensuring that the rotations are accomplished around the centers of the optical surfaces. Fine adjustment screws are used to move the off-axis parabolas thanks to lever arm. The manual screws can be substituted by motorized actuators if required at a later stage.

| Alignment requirements | | Lateral translation | Defocus | Tilt | Roll angle |
|---|---|---|---|---|---|
| **Star and Planet Fibers (SF, PF)** | Accuracy<br>Stability | 1 µm<br>0.02 µm | 10 µm<br>0.5 µm | 120 arcsec<br>5 arcsec | 1 deg.<br>1 deg. |
| **Star and Planet Mirrors (SM, PM)** | Accuracy<br>Stability | 100 µm<br>0.02 µm | 100 µm<br>0.1 µm | 10 arcsec<br>0.1 arcsec | 1 deg.<br>100 arcsec |
| **Beamsplitter (BS)** | Accuracy<br>Stability | 500 µm<br>500 µm | 500 µm<br>1 µm | 10 arcsec<br>0.1 arcsec | 1 deg.<br>1 deg. |
| **Focusing Mirror (FM)** | Accuracy<br>Stability | 2 µm<br>0.02 µm | 10 µm<br>0.1 µm | 10 arcsec<br>0.1 arcsec | 1 deg.<br>1 deg. |
| **Exozodi Mirror (EZM)** | Accuracy<br>Stability | 1 mm<br>100 µm | 1 mm<br>100 µm | 1 deg.<br>10 arcmin | 1 deg.<br>10 arcmin |
| **Exozodiacal Cloud (EZC)** | Accuracy<br>Stability | 2 µm<br>0.02 µm | 10 µm<br>1 µm | 1 deg.<br>1 deg. | 1 deg.<br>1 deg. |

Table 3: Geometrical alignment requirements for mixing optics and EZC (yellow cells indicating the needed movement stages, either in translation or rotation).

## 4 SPS OPTO-MECHANICAL DESIGN

In this section are presented the most recent CAD views of the SPS, which is currently near the end of its fabrication. A general picture of the whole SPS system is shown in Figure 6, while Figure 7 gives some detailed views about the BS/EZM opto-mechanical arrangement used to illuminate the EZC plate (on the right side of the Figure), and of the optical enclosure of the mixing optics assembly (on the left side). This modular structure made of thin black aluminum sheets is of particular importance, since it prevents any light leak in direction of the main optical bench (excepting the nominal star, planet and EZC beams), thus ensuring that the measured nulling maps and reconstructed images will not be affected with unwanted parasitic light reflections. Also, the enclosure has been split into two fixed and moving parts (not shown on the Figures) in order to insert and remove it easily from the main thermal enclosure of the PERSEE interferometer.

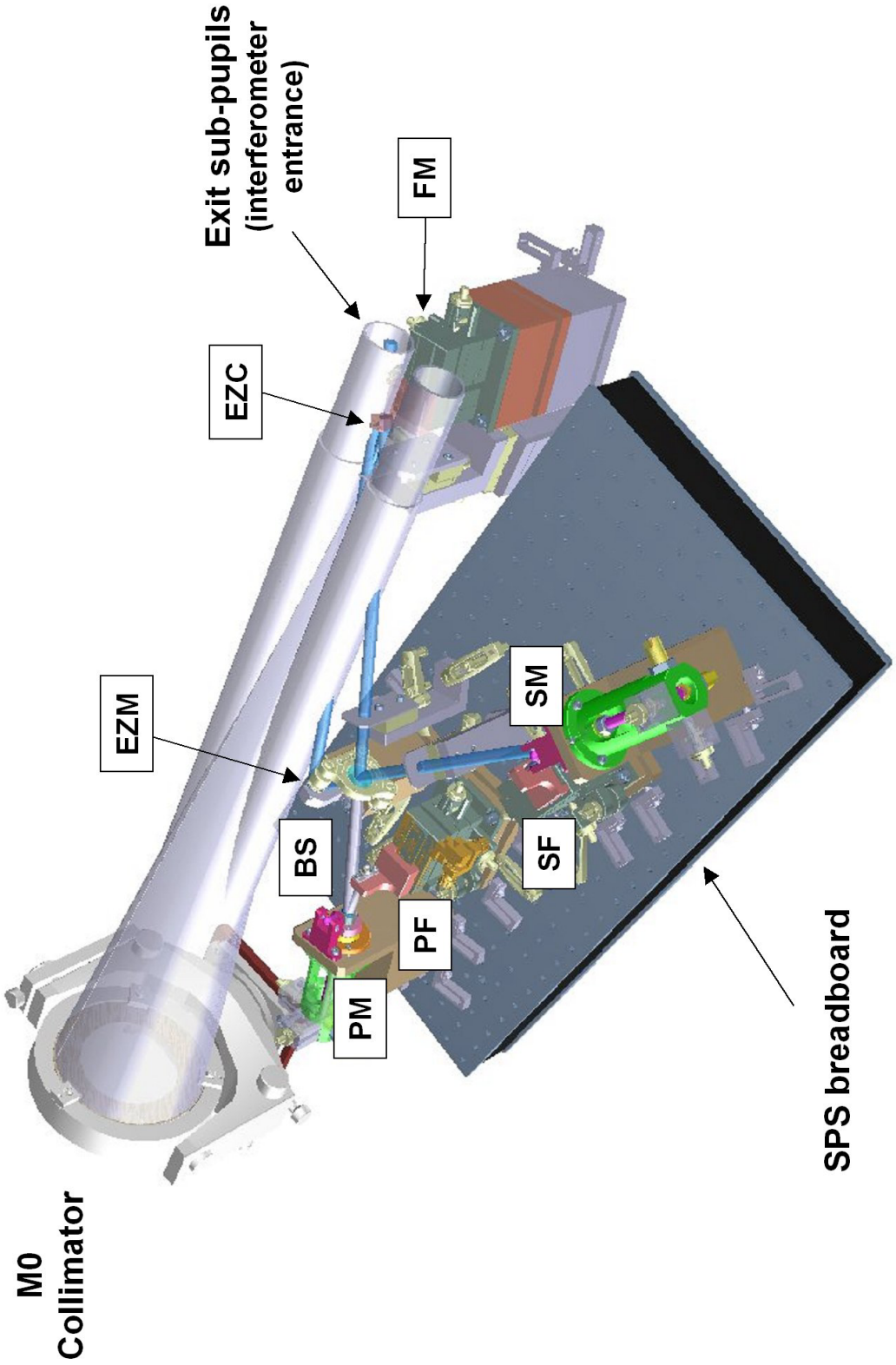


Figure 6: General CAD view of SPS module.

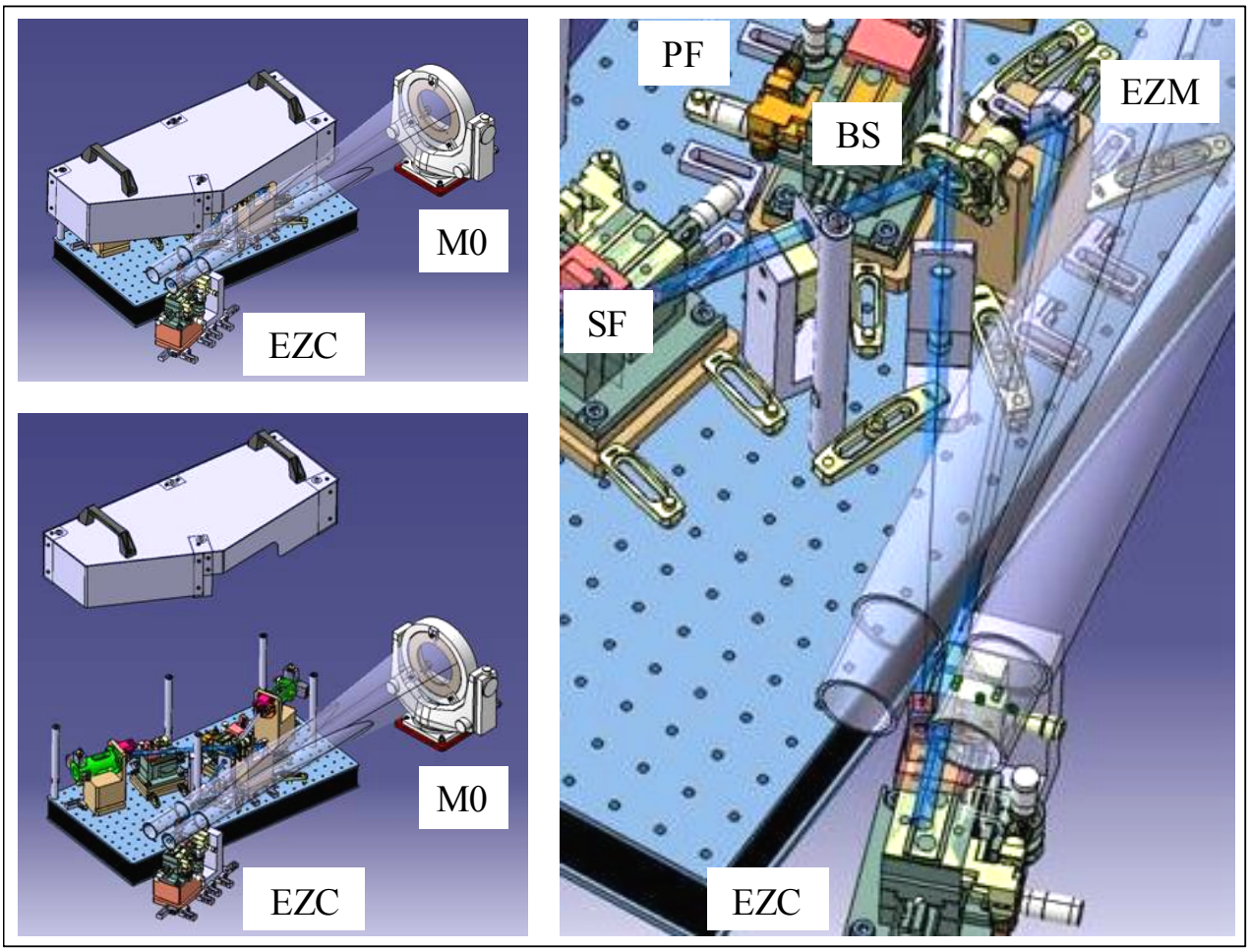


Figure 7: Detailed pictures of the SPS, showing the volume of the optical enclosure (left), and the BS/EZM arrangement focusing a pencil of light at the EZC plate (right).

## 5 CURRENT STATUS AND CONCLUDING REMARKS

In this paper was described the most recent extension of the nulling test bench PERSEE, jointly developed by CNES and five French institutes and companies. It essentially consists in enabling the present star simulator module to represent more complex astrophysical scenes, including a companion planet and a cloud of zodiacal debris. Hence the test bench will gain the capacity of testing and validating various types of data processing algorithms currently under study in order to reconstruct pseudo-images of the observed extra-solar systems. At the time of writing, a vast majority of the optical and mechanical components of this new star and planet simulator have already been defined, manufactured or procured from industry, and the rest is near the end of fabrication in OCA mechanical workshops. After elementary verification of their functional and alignment requirements, they will all be delivered and integrated at LESIA laboratory (Observatoire de Paris) in September 2011, at the sole and noticeable exception of the EZC plates that should be procured later. But it is likely that the first attempts of detecting the "Xenon planet" orbiting around its "super-continuum laser star" will be performed on the PERSEE test bench before the end of year 2011.

The authors would like to acknowledge all the funding organizations contributing to the development of the PERSEE test bench since five years, particularly CNES, ONERA and the French region Ile-de-France under convention I-06-201/R Sesame 2005.

## REFERENCES


[1] R.N Bracewell, R.H. MacPhie "Searching for non solar planets," Icarus 38, p. 136-147 (1979).

[2] A. Léger, J. M. Mariotti, B. Mennesson, M. Ollivier, J. L. Puget, D. Rouan, J. Schneider, "Could we search for primitive life on extrasolar planets in the near future ? The Darwin project," Icarus 123, p. 249-255 (1996).

[3] "TPF-I Science Working Group Report," JPL Publication 07-1, P. R. Lawson, O. P. Lay, K. J. Johnston and C. A. Beichman eds., Jet Propulsion Laboratory, California Institute of Technology, Pasadena, California (2007).

[4] W. Danchi, R. Barry, P. Lawson, W. Traub, S. Unwin, "The Fourier Kelvin Stellar Interferometer (FKSI): a review, progress report, and update," Proceedings of the SPIE 7013, n° 70132Q (2008).

[5] J.M. Le Duigou, M.Ollivier, A. Léger, F. Cassaing, B. Sorrente, B. Fleury, G. Rousset, O. Absil, D. Mourard, Y. Rabbia, L. Escarrat, F. Malbet, D. Rouan, R. Clédassou, M. Delpech, P. Duchon, B. Meyssignac, P.Y. Guidotti, N. Gorius, "Pegase: a space-based nulling interferometer," Proceedings of the SPIE 6265, n° 62651M (2006).

[6] F. Cassaing, J.M. LeDuigou, J.P. Amans, M. Barillot, T. Buey, F. Hénault, K. Houairi, S. Jacquinod, P. Laporte, A. Marcotto, L. Pirson, J.M. Reess, B. Sorrente, G. Rousset, V. Coudé du Foresto, M. Ollivier, "Persee: a nulling demonstrator with real-time correction of external disturbances," Proceedings of the SPIE 7013, n° 70131Z (2008).

[7] K. Houairi, S. Jacquinod, M. Barillot, F. Cassaing, J.-M. Le Duigou, F. Hénault, J. Lozi, M. Ollivier, J.-M. Reess, "Performance of the cophasing system of PERSEE, a dynamic nulling demonstrator", in *Pathways towards habitable planets* (Barcelone Parthways, 2009).

[8] S. Jacquinod, M. Barillot, F. Cassaing, J.-M. Le Duigou, F. Hénault, K. Houairi, J. Lozi, M. Ollivier, J.-M. Reess, "PERSEE: a nulling interferometer with dynamic correction of external perturbations," in *Pathways towards habitable planets* (Barcelone Parthways, 2009)

[9] F. Hénault, P. Girard, A. Marcotto, N. Mauclert, C. Bailet, J.-M. Clausse, D. Mourard, Y. Rabbia, A. Roussel, M. Barillot, F. Cassaing, J.-M. Le Duigou, "Review of OCA activities on nulling testbench PERSEE," Proceedings of the SPIE 7734, n° 77342U (2010).

[10] J. Lozi, F. Cassaing, J.M. Le Duigou, K. Houairi, B. Sorrente, J. Montri, S. Jacquinod, J-M Reess, L. Pham, E. Lhomé, T. Buey, F. Hénault, A. Marcotto, P. Girard, N. Mauclert, M. Barillot, V. Coudé du Foresto, M. Ollivier, "PERSEE: Experimental results on the cophased nulling bench," Proceedings of the SPIE 7734, n° 77342M (2010).

[11] J. Lozi et al, "Current results of the PERSEE testbench: the cophasing control and the polychromatic null rate," in these proceedings.

[12] P. Bély, L. Petro, R. Burg, L. Wade, C. Beichman, J. Gay, P. Baudoz, Y. Rabbia, J.-M. Perrin, "The Exo-Zodiacal disk Mapper: a space interferometer to detect and map zodiacal dust disks around nearby stars," Experimental Astronomy 9, p. 189-204 (1999).

[13] O. Absil, D. Defrère, A. Roberge, J.-C. Augereau, V. Coudé du Foresto, C. Hanot, C. Stark, J. Surdej, "Direct imaging of Earth-like planets: why we care about exozodis," Proceedings of the SPIE 7734, n° 77340L (2010).

[14] S. Martin, A. Booth, "Strong starlight suppression sufficient to enable direct detection of exoplanets in the habitable zone," Astronomy and Astrophysics 511, p. L1-L4 (2010).

[15] F. Hénault, "Computing extinction maps of star nulling interferometers," Optics Express 16, n° 7, p. 4537-4546 (2008).

[16] F. Hénault, "Fine art of computing nulling interferometer maps," Proceedings of the SPIE 7013, n° 70131X (2008).

[17] F. Hénault, "Simple Fourier optics formalism for high angular resolution systems and nulling interferometry," JOSA A 27, p. 435-449 (2010).

[18] C. Ruilier, F. Cassaing, "Coupling of large telescope and single-mode waveguides: application to stellar interferometry," JOSA A 18, p. 143-149 (2001).